AIAA JOURNAL
Vol. 35, No. 7, July 1997

Effects of Coriolis Force on Flow in Rotating Diffusers

Hide S. Koyama* and Kuniharu Uchikawa†
Tokyo Denki University, Tokyo 101, Japan
and
Hani H. Nigim‡
Birzeit University, Birzeit, Palestine

To investigate the coupled effects of secondary flow, stability (or instability) due to Coriolis force, and adverse pressure gradient on the flow in a rotating diffuser of low aspect ratio, quantitative experiments were performed. The diffuser had parallel end walls and straight side walls, which could vary its included angle up to 18 deg. Pressure, mean velocity, and turbulence intensity were measured with a pressure transducer, hot-wire anemometers, and a transmission system of electrical signals from a rotating apparatus to the stationary system. Experimental results indicate the formation of a stable large separated flow region on the suction side and a through-flow region on the pressure side. The flow pattern was steady, and once the separation occurred, the change of the angular velocity had little or no effect on the mean velocity and turbulence intensity profiles at the midheight of the rotating diffuser.

Nomenclature

C_p	= static pressure coefficient
H_{12}	= shape factor
p	= static pressure
p_t	= total pressure
Re	= Reynolds number, $U_m x/\nu$
Ri	= Richardson number
Ro	= rotation number, $\omega x/U_m$
r	= local radius
u, U_m, U_p	= mean velocities
$u\prime$, $v\prime$	= root mean square of fluctuating velocities
W	= width of diffuser
x, y, z	= coordinates
γp	= percent of time of downstream flow
δ	= boundary layer thickness
δ_1	= displacement thickness
θ	= diffuser included half angle
ν	= fluid kinematic viscosity
ρ	= fluid density
ω	= angular velocity

Subscripts

s	= suction side
p	= pressure side
1	= diffuser inlet condition

Introduction

MANY investigations concerning flow mechanism in the passages of centrifugal impellers have been reported over the years.[1–4] Recently, a low-speed centrifugal compressor facility was designed and built by the NASA Lewis Research Center. The purpose of this facility is to obtain detailed flowfield measurements for computational fluid dynamic code assessment and fundamental flow physics research. Preliminary experimental investigation results of inlet and exit flow uniformity and measurement repeatability were reported by Hathaway et al.[5] The computational fluid dynamic models used for analysis of the low-speed centrifugal compressor flowfield may not have correctly predicted the magnitudes of the flow parameters.

Received Feb. 24, 1996; revision received March 10, 1997; accepted for publication March 13, 1997.

*Professor, Department of Mechanical Engineering, 2-2 Kanda-Nishikicho, Chiyoda-ku.

†Specialist Engineer, Department of Mechanical Engineering, 2-2 Kanda-Nishikicho, Chiyoda-ku.

‡Associate Professor, Department of Mechanical Engineering, P.O. Box 14, via Israel. Associate Fellow AIAA.

The flow mechanism within actual centrifugal impellers is not yet understood completely because of the complexity of the flow that is affected by the coupled effects of the adverse pressure gradient, the rotation and the streamline curvatures of hub and shroud from the axial to the radial direction, and blades in the tangential direction. To elucidate this problem, various approaches have been carried out. It is common knowledge that the stability of shear flow and the secondary flow play important roles in the rotating system. For example, the motion of fluid particles is stabilized in the boundary layer on the suction side (parallel to the axis of rotation) of the rotating rectangular channel, whereas on the pressure side the motion of fluid particles is destabilized. Secondary flows from the pressure side to the suction side arise in boundary layers known as Ekman layers on the top and bottom walls (perpendicular to the axis of rotation) because of the imbalance between the Coriolis force and the pressure force. Therefore, these phenomena are generally referred to as the stabilizing (or destabilizing) effect and the secondary flow effect of Coriolis force, respectively.

Moore[6] investigated the effects of rotation, secondary flow, and adverse pressure gradient on flow in a rotating diffuser with aspect ratio 1:1 at the inlet. Experimental results indicated that, at high flow rates, the boundary layer attached on the pressure side, whereas a large wake was formed on the suction side of the diffuser. The suction side boundary layer thickened as the fluid transported toward the suction side concentrated in a large wake region. However, secondary flow through the pattern was not symmetrical and no reverse flow was measured in this wake region; hence, the flow was not separated in the two-dimensional sense. Moore suggested that the entrainment at the edge of the wake was small compared to the crossflows into the region from the top and bottom walls.

Rothe and Johnston[7] and Johnston[8] reported experiments concerning the effects of rotation on the flow in a rotating diffuser that was attached to the end of the long channel of aspect ratio 7.2:1. The results showed that the flow always was separated from the suction side and downstream of the separation point; a shear layer marked a sharp boundary between a through-flow and a separated region. The separated region was steady compared with that found in a stalled stationary diffuser. Flow visualization results showed that, on the free shear layer between the through-flow and the separated region, there was little mixing or entrainment.

Sturge[9] investigated the influence of rotation on the growth and separation of the turbulent boundary layers on the side walls of a rotating diffuser of aspect ratio 2:1 at the inlet. The growth and separation of the boundary layer on the suction side, the subsequent development of a wake including reverse flow on that side, and the thinning of the boundary layer on the pressure side that were found were attributed mainly to secondary flows on the end walls. No direct evidence of the expected influence of the Coriolis force on

boundary-layer stability was found because on the suction side the turbulence intensity increased to a high value of about 15% in the middle of the boundary layer.

Kikuyama et al.[10,11] investigated the effects of rotation on the flow in rotating conical and cross-section diffusers of different included angles. From the experimental results, it was found that the flow patterns in the diffusers were changed strongly by the rotation number. The separation point moved toward the inlet of the diffuser, and the pressure energy recovery decreased with increasing rotation number. With increasing included angle, the turbulence intensity and mean velocity gradient increased near the pressure side wall but decreased near the suction side wall.

The objective of the present study is to investigate the secondary flow effect and stabilizing (or destabilizing) effects of Coriolis force on the flow in a rotating diffuser of low aspect ratio and to offer reliable experimental data on mean velocity and turbulence quantities that are desirable in numerical simulations of rotating diffuser flow. Detailed measurements were performed with a rotating wind tunnel. An important difference between the present experiment and those by Moore,[6] Sturge,[9] and Kikuyama et al.[11] is the inlet and exit flow conditions.

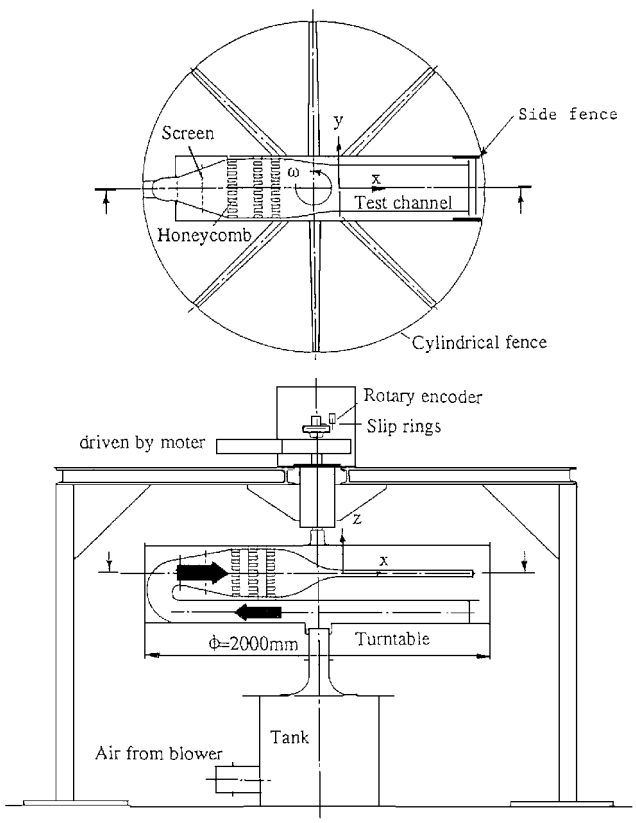

Fig. 1 Denki University, Tokyo, rotating wind tunnel.

Apparatus and Instrumentation

To study the stability and secondary flow effects of the Coriolis force on a rotating shear layer, a rotating wind tunnel was designed by Koyama et al.[12] A small wind tunnel was mounted on a turntable 2 m in diameter, which was rotating about a vertical axis at a considerable speed. Although the tunnel could be rotated in either direction, most of the experiments were performed for counterclockwise rotation as shown in Fig. 1. Air, delivered to the rotating duct by a fan blower, flowed through the rectification section and the symmetrical converging nozzle of contraction ratio 7.5:1 into the test channel. Rectification was secured by means of layers of honeycomb flow straighteners interspersed with screens. A test channel having a cross section 40 mm high $\times$ 280 mm wide and a length of 760 mm was attached to the end of the convergent nozzle. Flow in a rotating single channel, especially of low aspect ratio, is affected by crossflow, which is equal to the circumferential velocity at the channel exit.[13] To eliminate this obstructive influence in the study of Coriolis force effects, a fence 40 mm long $\times$ 110 mm high was installed on both sides of the test channel exit, and the rotating wind tunnel was covered with a cylindrical fence rotating at the same rotational speed of the wind tunnel. To obtain the turbulent boundary layers, two tripping wires with diameters of 1.0 and 1.5 mm were installed on the surfaces at the inlet and 75 mm upstream of the test channel. To construct a diffuser, two streamlined side walls were put in the test channel as shown in Fig. 2. The side walls could be pivoted around axes a–a as shown to maintain the same geometry upstream of the diffuser inlet, and the included angle 2θ could be varied continuously up to 18 deg. The experiments described here used 5, 10, and 15 deg. The diffuser had an aspect ratio of 1:2 at the inlet and a length of 660 mm. Arrays of static pressure taps were provided on the side wall surfaces and the bottom wall surface of the diffuser.

The pressure was sensed by a pressure transducer (Sankei Engineering, DPX10). Constant-temperature hot-wire anemometers (Dantec Electronik, 56C01, 56C17, and 56N21) and a single hot-wire sensor with a 5-μm tungsten wire were used for measurements of the mean velocity and turbulence intensity. A tandem hot-wire sensor was used to measure the unsteady reverse flow in the separated region and the percentage of downstream flow time. The hot-wire probe or pitot tube was traversed continuously by a traversing mechanism driven by a stepping motor while the wind tunnel was rotating. Power for operation of the hot-wire anemometer, the pressure transducer, and the traversing mechanism, as well as control signals, was transmitted through the rotating slip rings (Michigan

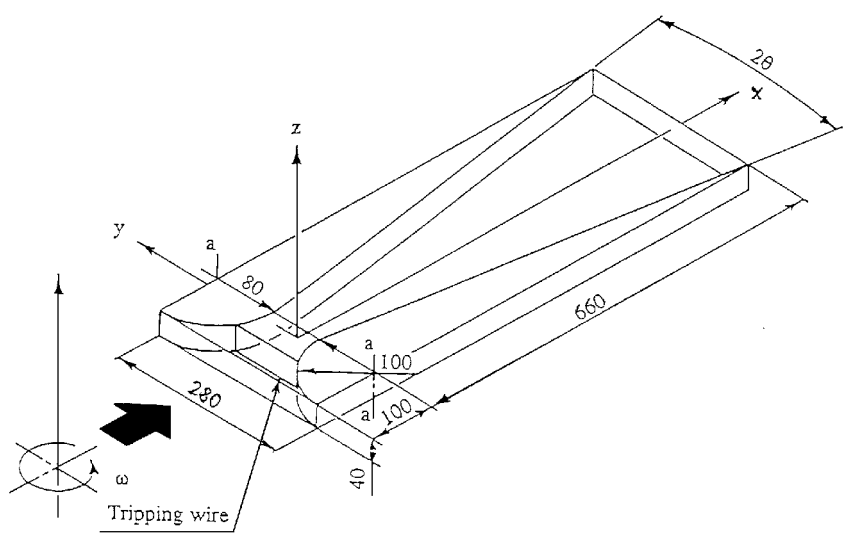

Fig. 2 Geometry and coordinate axes of rotating diffuser. Dimensions are in millimeters.

Scientific Co., SR20M). Control units of the hot-wire anemometer were mounted on the turntable. A new transmission system of hot-wire signals from the rotating system to the stationary system was designed to immunize the electrical noise, because the signals must be sent through a very noisy environment to the stationary system for further processing. Details of the signal transmission system used in the present experiment have been reported by Koyama et al.[12]

Experimental Results and Discussions

Reynolds number and rotation number, which is a measure of the Coriolis force relative to the inertia force, were formed utilizing x, the distance from the inlet of the diffuser:

$$Re = U_m x/\nu \tag{1a}$$

and

$$Ro = \omega x/U_m \tag{1b}$$

where U_m is the local mean velocity across the cross section and ω is the angular velocity of the diffuser. Measurements of mean velocity and turbulence intensity were made at six locations at 100-mm intervals under conditions of diffuser inlet velocity equal to 10.0 m/s; $\omega = 0.0$, 5.2, and 10.5 rad/s; and $2\theta = 5$, 10, and 15 deg. In the experiments described here, global Re and Ro at the exit of the diffuser of $2\theta = 15$ deg are 1.26×10^5 and 2.42, respectively.

Hill and Moon,[14] Moon,[15] and Wagner and Velkoff[16] put forth a great effort to achieve a uniform velocity profile at the inlet of a rotating test channel for all angular velocities of the wind tunnel. In the present experiments, however, no efforts were made to get a uniform velocity at the diffuser inlet. The system rotation imposes a linear velocity gradient along the transverse direction at the inlet where the flow is potential. Figure 3 shows the inlet flow conditions of the rotating diffusers. It shows the profiles of mean velocity u/u_1, where u_1 is the reference mean velocity measured in the midheight of the diffuser at the inlet, i.e., $x = 0.0$, turbulence intensity u/u_1, and reduced total pressure $p_t^*[= p_t - (\rho r^2\omega^2/2)]/p_{t1}^*$, where p_t is total pressure, r is the local radius from the axis of rotation, and p_{t1}^* is reduced total pressure in the center of the diffuser at the inlet for the cases of $\omega = 0.0$, 5.2, and 10.5 rad/s, and $2\theta = 15$ deg. For counterclockwise rotation, the upper line at $y/W_1 = 0.50$, where W_1 is the width of the diffuser at the inlet, is the suction side surface of the rotating diffuser and the lower line at $y/W_1 = -0.50$ is the pressure side surface. As ω increased, the boundary-layer thickness increased on the suction side and slightly decreased on the pressure side.

These phenomena might be due to the secondary flows arising in the boundary layers on the top and bottom walls of the converging section upstream of the diffuser inlet. Although a weak increasing tendency could be seen, the freestream-turbulence intensities were less than 0.4% for both the stationary and rotating cases. Overshoots of velocity were observed near the walls at the inlet of the diffuser. However, it was fully noticeable that the total pressures between the

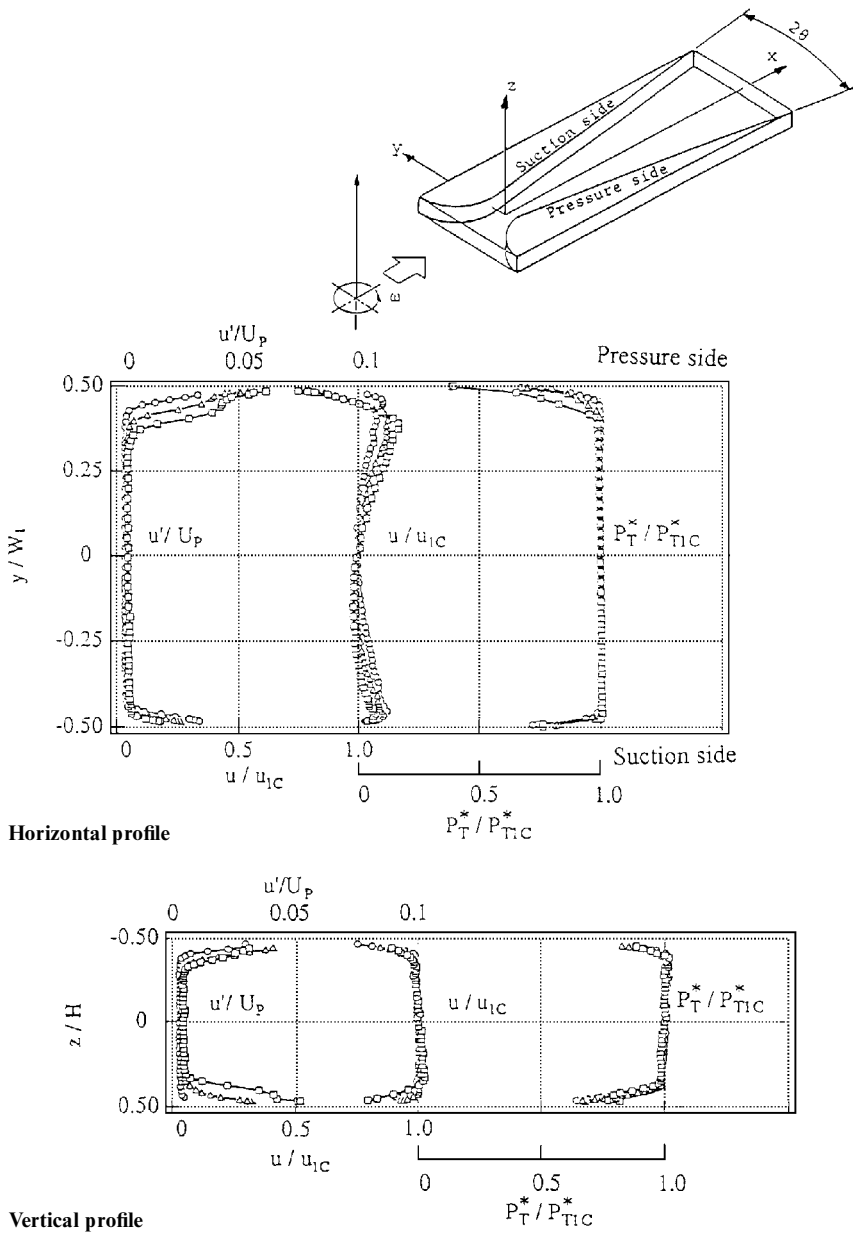

Fig. 3 Profiles of mean velocity, turbulence intensity, and reduced total pressure of rotating diffusers: ○ 0 rad/s; △, 5.2 rad/s; and □, 10.5 rad/s.

side walls for both the stationary and rotating cases were constant outside the boundary-layer regions, i.e., the flows were potential. Boundary-layer thickness at the inlet exerts a large influence on the efficiency of pressure recovery of even a stationary diffuser. The inlet blockage factor was about 0.03.

From the experimental results for the stationary diffusers, it was found that the boundary-layer developments were promoted on the side walls of the stationary diffusers because of the adverse pressure gradient along the walls. Points of inflexion of the velocity profile were observed in the boundary layer at the exit for $2\theta = 10$ deg and downstream of $x/W_1 = 3.75$ for $2\theta = 15$ deg. For the cases of $2\theta = 5$ and 10 deg, the velocity profiles were almost symmetrical over the width of the diffusers. Although the lack of symmetry could be seen at the exit of $2\theta = 15$ deg, frequent oscillation of the flow from one side to the other was not observed.

The analogy between density stratified, curved streamline, and rotating turbulent flows has been discussed by Bradshaw.[17] As an appropriate measure of the local stability for the case of rotating, parallel shear flow the gradient Richardson number was defined as follows:

$$Ri = -2\omega \frac{\partial u/\partial y - 2\omega}{(\partial u/\partial y)^2}$$

$$= S(1 + S) \tag{2}$$

where S is $-2\omega/(\partial u/\partial y)$, which represents the ratio of the local Coriolis force $-2\omega u$ to the inertia force $u(\partial u/\partial y)$.

Profiles of u/u_1, $u\prime/U_p$, where U_p is hypothetical velocity extrapolated from the velocity profile between the boundary layer edges δs and δp, for the case of $\omega = 10.5$ rad/s, and $2\theta = 15$ deg, are shown in Fig. 4. Richardson number, as defined by Eq. (2), and percentage downstream flow time γp between the side walls at midheight of the rotating diffuser are also shown in Fig. 4. Squares represent the profiles measured by the single hot-wire sensor, and solid circles represent the profiles by the tandem hot-wire sensor. As ω and 2θ increased, boundary-layer development was promoted on the suction side and suppressed on the pressure side, in comparison with the case of a stationary diffuser. The slope of the velocity profile increased in the vicinity of the pressure side wall and decreased on the suction side. These tendencies were exaggerated with increasing ω and x. For the case of $\omega = 10.5$ rad/s, the boundary layer separated at $x/W_1 = 5.00$ for $2\theta = 10$ deg and at $x/W_1 = 2.50$ for $2\theta = 15$ deg at the least. However, separation was not observed for the case of $2\theta = 5$ deg. The measurements of secondary flows in rotating diffusers have been carried out by Moore,[6] Sturge,[9] and Kikuyama et al.[10] Those experiments clearly indicated the presence of two longitudinal vortices that extended the length of the channel. It seems that the same type of longitudinal vortices also arise in the rotating diffuser described here. Consequently, the secondary flows in the end wall boundary layers may have relatively strong effects on the overall flow, especially on the boundary-layer development on the suction side of the diffuser.

Consider a transient state flow in a diffuser that is rotating toward an established constant angular velocity from the rest. As the angular velocity increases, the boundary-layer development is promoted on the suction side and is suppressed on the pressure side because of the secondary flows arising in the top and bottom wall boundary layers. The fully developing and retarded boundary layer separates only from the suction side wall because of the coupled effects of secondary flow and stability; it never separates from the pressure side because of the coupled effects of secondary flow and instability. Here, the secondary flow effect may be stronger than the instability effect. Once the incoming flow has separated from the suction side wall, the separated flow is steady, and a change of angular velocity has little or no effect on the mean velocity and turbulence intensity profiles at the diffuser midheight.

Figure 5 shows the profiles of u/u_1, $u\prime/U_p$, Richardson number, and γp between the side walls at $x/W_1 = 6.25$ for the case of $\omega = 10.5$ rad/s and $2\theta = 15$ deg. The flow was divided into three regions: a reverse flow (wake) on the suction side and a through-flow (jet) on the pressure side, with a shear flow between them. The point where $\gamma p = 50$ corresponded virtually to the edge of the

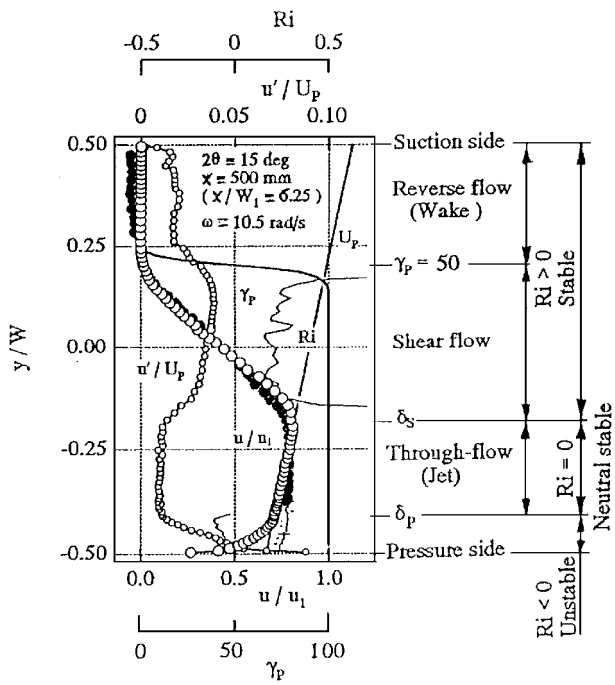

Fig. 5 Reverse flow, shear flow, and through-flow regions.

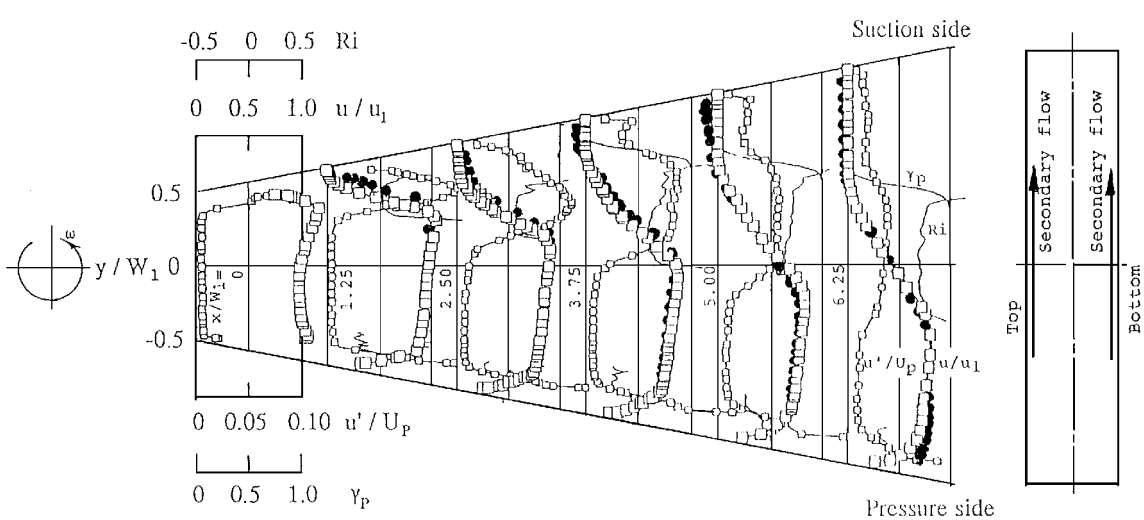

Fig. 4 Profiles of mean velocity, turbulence intensity, percentage downstream flow time, and Richardson number for the case of $2\theta = 15$ deg and $\omega = 10.5$ rad/s.

reverse flow region. In the reverse flow region, where γp was equal to zero, turbulence intensity was nearly constant. Ri was about 2.5 in the center portion of the shear flow region between the reverse flow and the through-flow. This value is enough to stabilize the shear flow, as demonstrated in the discussion about the relation between Richardson number and the degree of the stabilizing or destabilizing effect on the boundary-layer development in rotating low- and high-aspect ratio channels (see Fig. 6). In the shear flow region, similarity of mean velocity profile was observed. Moreover, the turbulence intensity decreased with increasing the angular velocity for the same included angle because the production of turbulent shear stress was suppressed because of the stabilizing effect. The ratio of the production of Reynolds shear stress with rotation to that without is equal to $1 + \omega(u'^2/v'^2 - 1)/(\partial u/\partial y)$, where v' is a root-mean-square value of the fluctuating velocity component in the y direction. The ratio of Reynolds normal stresses u'^2/v'^2 is larger than unity in a general turbulent boundary layer. Therefore, the production of Reynolds shear stress decreases in the stabilized shear layer.

Theoretical investigations on the stability of boundary-layer flow and channel flows subject to rotation have shown that the flow on the pressure side ($Ri < 0$) is destabilized. In contrast, the flow on the suction side ($Ri > 0$) is stabilized. From the distribution of the Richardson number in the boundary layer, however, it may be not easy to estimate the degree of stabilizing or destabilizing effects on the developing turbulent boundary layer subject to rotation. Koyama and Ohuchi[18] studied the stabilizing and destabilizing effect isolated from the secondary flow effect on the two-dimensional boundary layer developing on the central portion of the side walls of a rotating straight channel of aspect ratio 7:1. Koyama et al.[19] also studied the coupled effects of secondary flow and stability (or instability). From comparison of these experimental results under the same conditions, inlet velocity equal to 10.0 m/s and $\omega = 10.5$ rad/s, it was found that for low aspect ratio the secondary flows arising in the top and bottom wall boundary layers convey fluid of lower velocity and higher turbulence intensity to the suction side, where it accumulates and forms a rapidly developing turbulent boundary layer, in contrast with the original stabilizing effect observed for the case of high aspect ratio. Consequently, the boundary layer on the suction side of the straight channel of low aspect ratio is strongly stabilized because of the decrease of the velocity gradient.

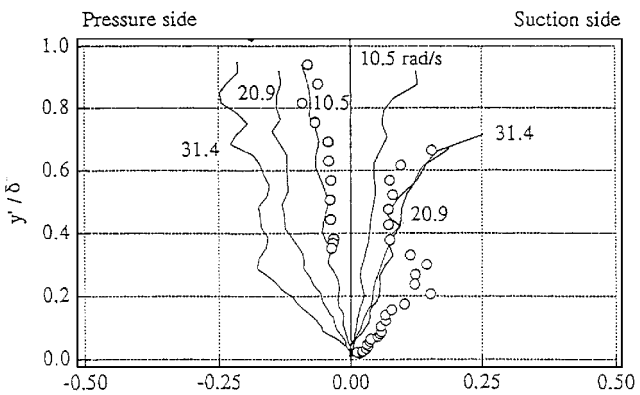

a) Rotating straight channel

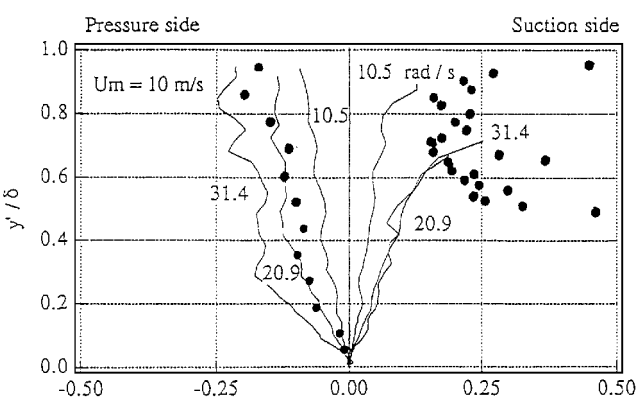

b) Rotating diffuser flows

Fig. 6 Distributions of Richardson number: ——, two-dimensional boundary layers, $\partial p/\partial x \cong 0$; ○ three-dimensional boundary layers, $\partial p/\partial x \cong 0$, 10.5 rad/s; and ● three-dimensional boundary layers, $\partial p/\partial x > 0$, 10.5 rad/s.

Distributions of Richardson number in the boundary layers of straight channels are shown in Fig. 6a, where the two cases are compared. The solid lines represent the two-dimensional boundary layers in a rotating channel of high aspect ratio; in this case, the flows were affected only by the stability effect, and the circles represent the three-dimensional boundary layers in a channel of low aspect ratio, where the flows were affected by the coupled effects of stability and secondary flow. In Fig. 6a, y' is the distance from the side wall and δ is the boundary-layer thickness. For the case of high aspect ratio, the stability effect on the mean velocity and turbulence intensity profiles was negligible on the suction and pressure sides at the same angular velocity, equal to 10.5 rad/s, but a large change was observed at $\omega = 31.4$ rad/s. From these comparisons, it is suggested that for the case of low aspect ratio at relatively low angular velocity, secondary flows in end walls have very strong effects on the boundary-layer development on the side walls of a rotating channel. Especially on the suction side, as there is increasing boundary-layer thickness, the flow may be stabilized substantially because the value of the Richardson number was higher than that at $\omega = 31.4$ rad/s near the wall, where the turbulence production shows a maximum. These considerations can be applied to the flow in the rotating diffuser of low aspect ratio. In Fig. 6b, the lines represent the same as Fig. 6a, and the symbols represent the cases of the three-dimensional boundary layers at $x/W_1 = 6.25$ of the present diffuser for the case of $\omega = 10.5$ rad/s and $2\theta = 15$ deg. On the suction side, the flow is stabilized substantially because the values of the Richardson number are extremely high, especially near the wall.

The velocity gradient of the potential flow within a rotating parallel channel is equal to 2ω in the plane normal to the rotation axis. Usually, actual flow consists of boundary layers accompanied by a potential core within rotating side walls in a constant-area straight channel. As a fundamental idea, if the mean velocity and turbulence quantities in the turbulent boundary layers on the side walls are nondimensionalized by the corresponding velocity of the potential flow, one can evaluate them under the same criterion for the rotating and nonrotating cases. Therefore, in this paper, the hypothetical velocity U_p, which was extrapolated from the velocity profile outside the boundary layer (see Fig. 5), was used as a reference velocity for calculations of the boundary-layer integral thicknesses.

Figure 7 shows the variation of the displacement thickness δ_1 and the shape factor H_{12} of the boundary layers on the side walls of stationary and rotating diffusers with $2\theta = 5$, 10, and 15 deg. On the suction side, the development of the boundary layer was promoted in the streamwise direction; development was suppressed on the pressure side. Especially on the pressure side for the case of $2\theta = 15$ deg, the thicknesses were nearly constant in the streamwise direction. The H_{12} also had a constant downstream of the location $x/W_1 = 1.25$ and is nearly independent of the included angle and the angular velocity. The freestream was deflected toward the pressure side because of the strong effect of displacement on the suction side. The magnitudes of these phenomena were not linearly proportional to the angular velocity. It is important to determine the onset of separation. The point of separation is defined as the velocity gradient at the wall equal to zero. Moore[6] concluded that the skin friction approached zero as the suction side boundary layer thickened to a large wake flow, with a shape factor of approximately 3.8. However, no reverse flow was measured in the wake region; hence, the flow was not separated in the two-dimensional sense. In the present results, the shape factor was approximately 6.6 at the location $x/W_1 = 2.5$ for the case of $2\theta = 15$ deg and at $\omega = 10.5$ rad/s, where a reverse flow was not observed. Probably, the shape factor at the onset of separation is dependent on the aspect ratio at the diffuser inlet. Rothe and Johnston,[7] in a study of a rotating diffuser of high aspect ratio, found that the end wall crossflows did not sweep into the wake region of low-speed fluid. Rather, the crossflows appear to be entrained by the free shear layer downstream of boundary-layer separation from the suction side. They emphasized that such

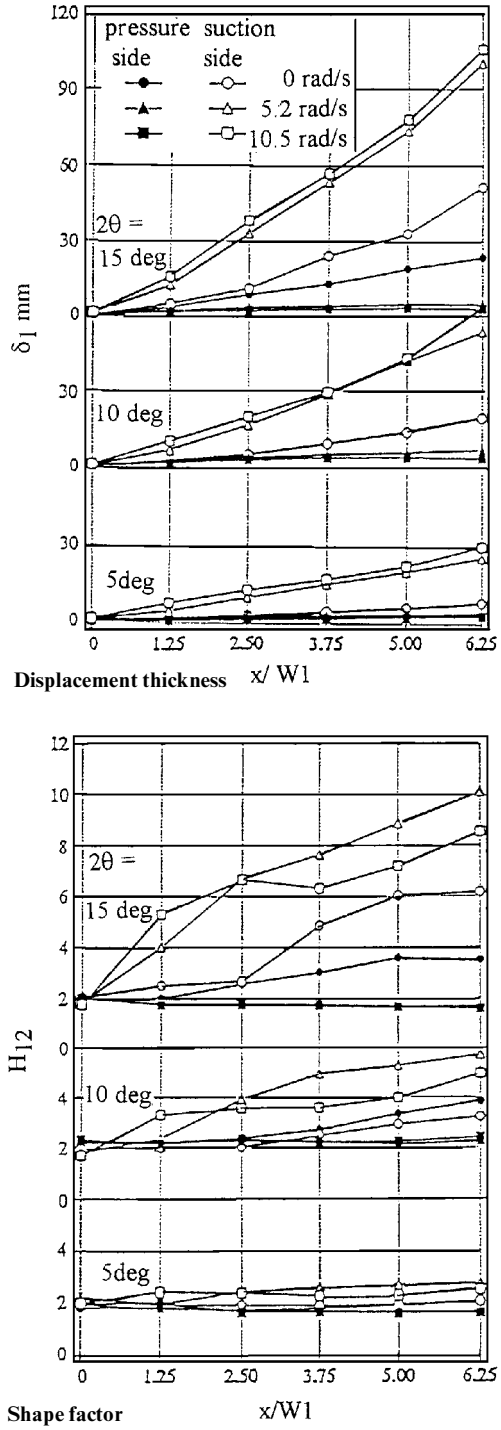

Fig. 7 Distributions.

observations in a high-aspect-ratio diffuser may not be representative of the crossflow patterns in low-aspect-ratio passages typical of centrifugal impellers.

Static pressure distributions were measured in the diffusers with $2\theta = 5$, 10, and 15 deg for $\omega = 0.0$, 5.2, and 10.5 rad/s. A local static pressure tap was connected by tubing to a pressure transducer, which was mounted on the turntable centerline. The transducer sensed a reduced static pressure $p^* = p - (\rho r^2 \omega^2/2)$, where p is static pressure. Figure 8 shows the distributions of the static pressure coefficient C_p, which is defined as

$$C_p = \frac{p^* - p_1^*}{\rho u_1^2/2} \tag{3}$$

where p_1^* is an averaged, reduced static pressure across the side walls at the inlet of the diffuser. For the case of $2\theta = 5$ deg, the distribution of C_p was virtually independent of ω However, as 2θ increased, the

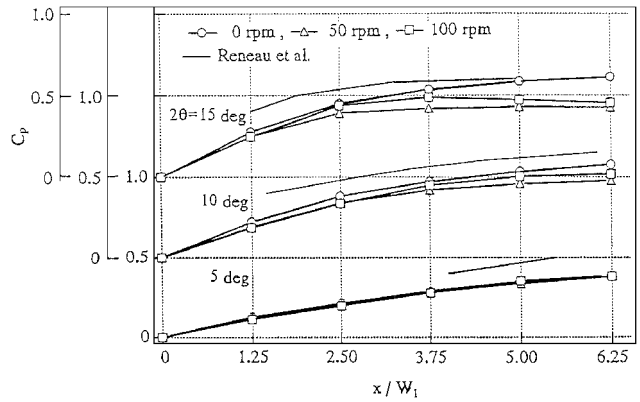

Fig. 8 Distribution of static pressure coefficient.

independence could not be maintained, and the influence of ω could be seen. The C_p of the stationary diffusers employed here was lower than that of the diffusers of high aspect ratio reported by Reneau et al.[20] This difference might be due to the shape of the cross section at the inlet of the diffuser.

Conclusions

Conclusions reached as a result of the present study may be summarized as follows.

1) As angular velocity increases, the boundary-layer development is promoted on the suction side and suppressed on the pressure side because of the secondary flows arising in the top and bottom wall boundary layers of the rotating diffuser of low aspect ratio. Eventually, the fully developed and retarded boundary layer separates only from the suction side wall because of the coupled effects of adverse pressure gradient, secondary flow, and stability; it never separates from the pressure side because of the coupled effects of secondary flow and instability, but the secondary flow effect may be stronger than the instability effect.

2) Once the oncoming flow is separated from the suction side wall, the separated flow pattern is steady because of the combined effects of secondary flow and stability because of Coriolis force. A change of angular velocity has little or no effect on the mean velocity and turbulence intensity profiles at the diffuser midheight. The flow is divided approximately into three regions, a through-flow (jet) on the pressure side, a reverse flow (wake) on the suction side, and a shear flow between them.

3) In the shear flow region, the turbulence intensity decreases with increasing angular velocity at the same included angle because the production of turbulent shear stress is suppressed because of the stabilizing effect of Coriolis force. Generally, these phenomena were not linearly proportional to the angular velocity.

Acknowledgments

This work was supported in part by a Grant-in-Aid for scientific research from the Center for Research, Tokyo Denki University. The authors express their thanks to N. Nawabuchi for his cooperation in carrying out the present experiments.

References

[1]Fujie, K., "Three-Dimensional Investigation of Flow in Centrifugal Impeller with Straight-Radial Blades," *Bulletin of the Japan Society of Mechanical Engineers*, Vol. 1, No. 1, 1958, pp. 42–49.

[2]Eckardt, D., "Detailed Flow Investigations Within a High-Speed Centrifugal Compressor Impeller," *Journal of Fluids Engineering*, Vol. 98, No. 3, 1976, pp. 390–402.

[3]Mizuki, S., Ariga, I., and Watanabe, I., "A Study on the Flow Mechanism Within Centrifugal Impeller Channels," American Society of Mechanical Engineers, Paper 75-GT-14, April 1979.

[4]Johnson, M. W., and Moore, J., "Secondary Flow Mixing Losses in a Centrifugal Impeller," *Journal of Engineering for Power*, Vol. 105, Jan. 1983, pp. 24–39.

[5]Hathaway, M. D., Wood, J. R., and Wasserbauer, C. A., "NASA Low-Speed Centrifugal Compressor for 3-D Viscous Code Assessment and Fundamental Flow Physics Research," American Society of Mechanical Engineers, Paper 91-GT-140, April 1991.

[6]Moore, J., "A Wake and an Eddy in a Rotating Radial Flow Passage, Part 1: Experimental Observations," *Journal of Engineering for Power*, Vol. 95, No. 3, 1973, pp. 205–212.

[7]Rothe, P. H., and Johnston, J. P., "Effects of System Rotation on the Performance of Two-Dimensional Diffusers," *Journal of Fluids Engineering*, Vol. 98, No. 3, 1976, pp. 422–430.

[8]Johnston, J. P., "Effects of System Rotation on Turbulence Structure—A Review Relevant to Turbomachinery Flows," *Sixth International Symposium on Transport Phenomena and Dynamics of Rotating Machinery* (Honolulu, HI), Vol. 2, Feb. 1996, pp. 1–17.

[9]Struge, D. P., "Flow in a Radial Impeller," Ph.D. Thesis, St. John's College, Univ. of Cambridge, Cambridge, England, UK, Feb. 1977.

[10]Kikuyama, K., Murakami, M., and Mastumoto, H., "Effects of Rotation on Diffuser Flow (Effects of Included Angles)," *Transactions of the Japan Society of Mechanical Engineers*, Vol. 45, No. 397, 1979, pp. 1257–1265 (in Japanese).

[11]Kikuyama, K., Murakami, M., and Gomi, K., "Effects of Coriolis Force on the Turbulent Boundary Layer with Pressure Gradients," *Transactions of the Japan Society of Mechanical Engineers*, Vol. 51, No. 472, 1985, pp. 4162–4169 (in Japanese).

[12]Koyama, H. S., Saito, T., and Ohuchi, M., "Vortex Street and Turbulent Wakes Behind a Circular Cylinder Placed in a Rotating Rectangular Channel," *Turbulent Shear Flows 6*, edited by L. J. S. Bradbury, J. C. Andre, J. Coustiex, F. Durst, B. L. Launder, F. W. Schmidt, and J. H. Whitelaw, Springer–Verlag, New York, 1989, pp. 283–298.

[13]Fowler, H. S., "The Distribution and Stability of Flow in a Rotating Channel," *Journal of Engineering for Power*, Vol. 90, No. 2, 1968, pp. 229–236.

[14]Hill, P. G., and Moon, I. M., "Effects of Coriolis Forces on the Turbulent Boundary Layer in Rotating Machines," Gas Turbine Lab., Rept. 69, Massachusetts Inst. of Technology, Cambridge, MA, June 1962.

[15]Moon, I. M., "Effects of Coriolis Forces on the Turbulent Boundary Layer in Rotating Machines," Gas Turbine Lab., Rept. 74, Massachusetts Inst. of Technology, Cambridge, MA, June 1964.

[16]Wagner, R. E., and Velkoff, H. R., "Measurements of Secondary Flows in a Rotating Duct," *Journal of Engineering for Power*, Vol. 94, Oct. 1972, pp. 261–270.

[17]Bradshaw, P., "The Analogy Between Streamline Curvature and Buoyancy in Turbulent Shear Flow," *Journal of Fluid Mechanics*, Vol. 36, Pt. 1, 1969, pp. 177–199.

[18]Koyama, H. S., and Ohuchi, M., "Effects of Coriolis Force on Boundary Layer Development," *Proceedings of the Fifth Symposium on Turbulent Shear Flows* (New York), 1985, pp. 21.19–21.24.

[19]Koyama, H. S., Tamura, E., and Saito, T., "Effects of Coriolis Force on Development Turbulent Channel Flow," *Proceedings of the Tenth Australian Fluid Mechanics Conference* (Melbourne, Australia), 1989, pp. 12.17–12.20.

[20]Reneau, L. R., Johnston, J. P., and Kline, S. J., "Performance and Design of Straight Two-Dimensional Diffusers," *Journal of Basic Engineering*, Vol. 89, No. 1, 1969, pp. 141–150.

S. Fleeter
Associate Editor